# CCC Annual Report

UIUC, August 19, 2015

## *Particle Capture in Mold including Effect of Subsurface Hooks*

**Kai Jin**

*Department of Mechanical Science & Engineering*
**University of Illinois at Urbana-Champaign**

# Objective

- Develop a model to include effects of hook on particle\bubble capture;
- Use advanced capture criterion[1-3] combined with hook capture mechanism to study the particle/bubble capture;

# Review of Inclusion Measurements (Baosteel Caster #4)

- Cut samples from as-cast slab: WF center, WF quarter, and NF;
- Mill away steel layer by layer.
- Examine bubbles with 35x optical microscope
- Record number and size distributions

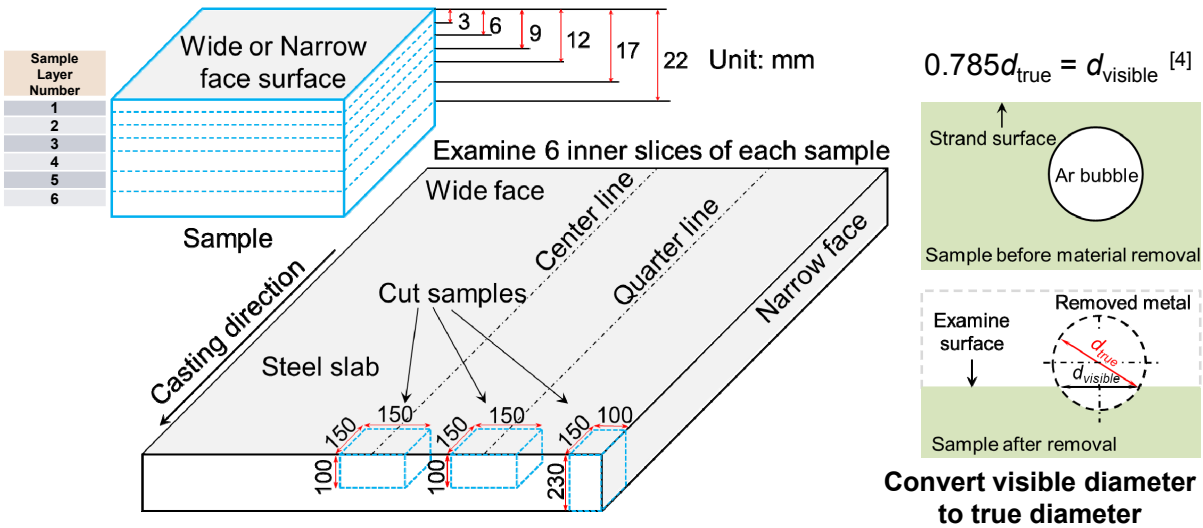




# Schematic of Hook Capture Mechanism

- A particle/bubble enters into a hook zone has three different possible fates
- $f_o$ is the mold oscillation frequency

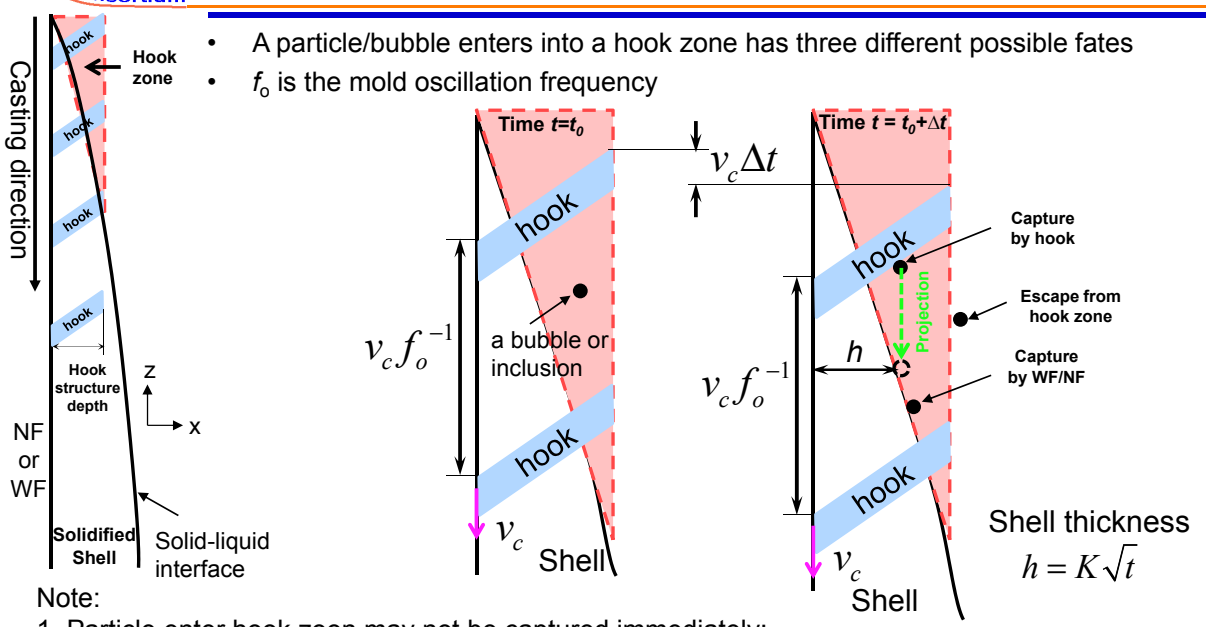


Note:

1. Particle enter hook zoon may not be captured immediately;
2. Particle may escape from the hook zone before it was captured;
3. Particles may hit the mushy zone front and be captured by WF/NF before captured by hook;
4. In post processing, project hook captured bubble vertically onto the shell

# Flow Chart of Hook Capture Mechanism

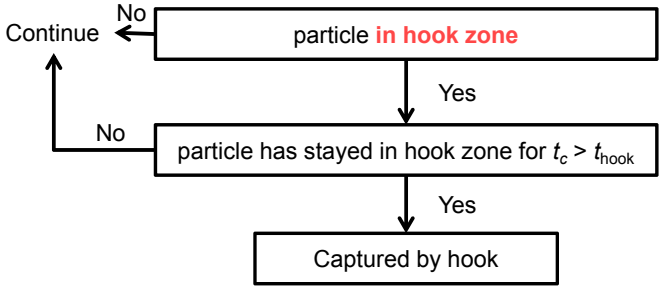


Particle re-entering hook zone

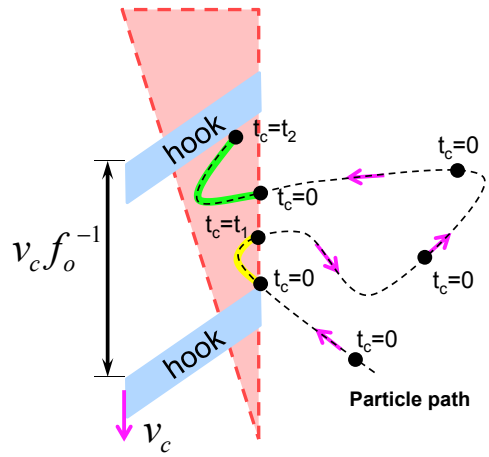


- $t_{hook}$ – a critical time, allows particle/bubble to travel before it is captured by the hook, on average, we take $t_{hook} = 0.5 f_o^{-1}$
- $t_c$ – time of a particle remained in the hood zone since it enters. Reset $t_c$ to 0 when particle cross the hook zone boundary (consider a particle re-entering the hook zone)

$t_1$: time taken for particle travel on yellow path; $t_1 < t_{hook}$, particle escaped from hook zone.
$t_2$: time taken for particle travel on green path; $t_2 > t_{hook}$, particle is captured by the hook.



# Add hook capture mechanism into advanced capture criterion [1-3]

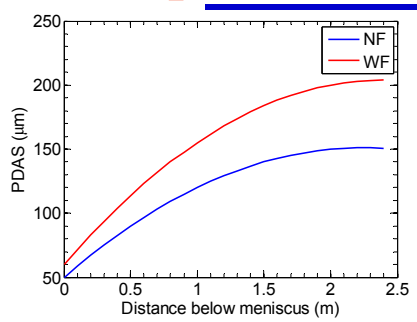


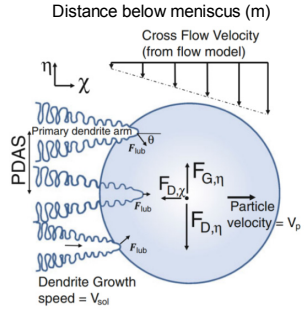


**A Bubble/Particle Touching 3 Dendrite Tips [3]**

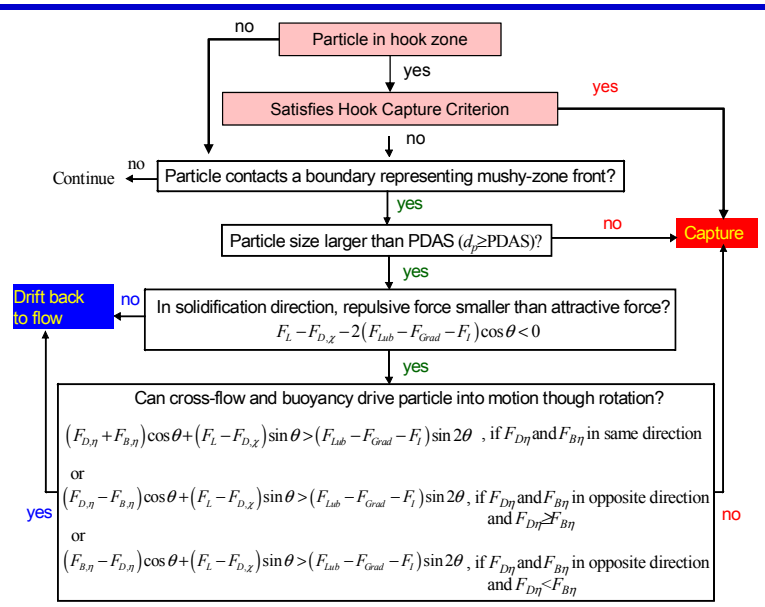


**Flow chart for Ar bubble/particle capture criterion [3]**

- Flow chart showing the modified and original advanced capture criterion;
- Hook capture mechanism are added in to FLUENT using UDF;

# Ar Bubble Distribution

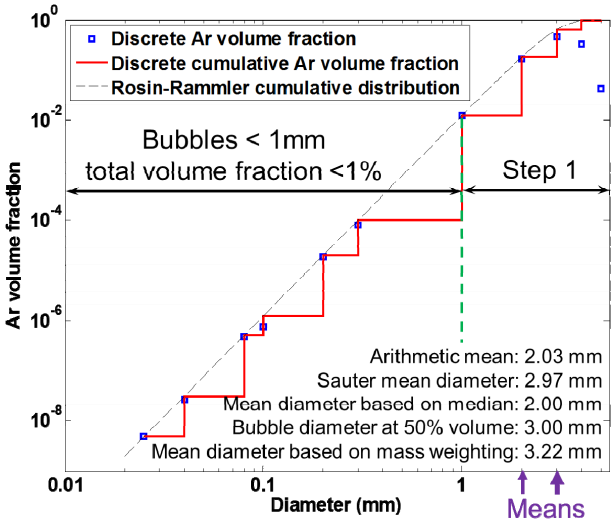


Bubbles < 1mm total <1% Volume fraction

Rosin-Rammler distribution, with mean diameter 3mm*

**Step–1**,
Obtain flow field with two-way coupled Euler-Lagrangian simulation:
using 5 largest groups of bubbles

**Step–2**,
Inject and track all 11 groups of all 250,000 bubbles.

**Repeat Step-2:** 10 times
~2.5 million bubbles tracked using each capture criterion

* Mean based on model by H. Bai & BG Thomas, MMTB, 2001



# Governing Equations

- Using Reynolds decomposition, steel velocity $\boldsymbol{u} = \boldsymbol{U} + \boldsymbol{u}'$
- The time averaged continuity and momentum equations for liquid steel (turbulence viscosity $\mu_t$ modelled by $k$-$\varepsilon$ model [5])

$$\nabla \cdot (\rho \boldsymbol{U}) + S_{\text{mass-sink}} = 0$$

$$\rho \cancel{\frac{\partial \boldsymbol{U}}{\partial t}}^{\,0} + \rho(\boldsymbol{U} \cdot \nabla)\boldsymbol{U} = -\nabla \bar{p}^* + \nabla \cdot \left[ (\mu + \mu_t)\left(\nabla \boldsymbol{U} + \nabla \boldsymbol{U}^T\right)\right] + \boldsymbol{S}_{\text{momentum-sink}} + \boldsymbol{S}_{\text{DPM}}$$

- Force balance equations for each individual bubble (diameter $d_p$, velocity $\boldsymbol{u}_p$, density $\rho_p$, mass $m_p$ and volume $V_p$)

$$m_p \frac{d\boldsymbol{u}_p}{dt} = \underbrace{\frac{m_p 18\mu}{\rho_p d_p^2}\frac{C_D}{24}(\boldsymbol{u} - \boldsymbol{u}_p)\overbrace{\frac{\rho d_p |\boldsymbol{u}_p - \boldsymbol{u}|}{\mu}}^{\mathrm{Re}_p}}_{\boldsymbol{F}_D} + \underbrace{0.5 m_p \frac{\rho}{\rho_p}\left(\frac{D\boldsymbol{u}}{Dt} - \frac{d\boldsymbol{u}_p}{dt}\right)}_{\boldsymbol{F}_v} + \underbrace{m_p \frac{\rho}{\rho_p}\frac{D\boldsymbol{u}_p}{Dt}}_{\boldsymbol{F}_p} + \underbrace{m_p \frac{\boldsymbol{g}(\rho_p - \rho)}{\rho_p}}_{\boldsymbol{F}_b}$$

$\boldsymbol{F}_D$ – drag force, and drag coefficient $C_D$ from Morsi [6];
$\boldsymbol{F}_V$ – virtual mass force; $\boldsymbol{F}_p$ – pressure gradient force; $\boldsymbol{F}_b$ – buoyancy/gravity

- Turbulence dispersion of particles: using Random Walk Model [7]

# Random Walk Model[7]

- Gaussian distributed random velocity fluctuation, *u'*, *v'* and *w'* are generated from

$$u' = \zeta\sqrt{\overline{u'^2}} \qquad \sqrt{\overline{u'^2}} = \sqrt{\overline{v'^2}} = \sqrt{\overline{w'^2}} = \sqrt{2k/3}$$

$\zeta$ – standard normal distribution random number.

- Eddy life time: $t_e = -t_L \ln(r)$ where $t_L = C_L \dfrac{k}{\epsilon} \approx 0.15\dfrac{k}{\epsilon}$

$r$ – uniformly distributed random number from 0 and 1.

- Eddy cross time $t_{cross} = -\tau \ln\left[1 - \dfrac{C_\mu^{4/3}\dfrac{k^{3/2}}{\epsilon}}{\tau\left|\vec{u} - \vec{u}_p\right|}\right]$

where $\tau = \dfrac{\rho_p d_p^2}{18\mu}$

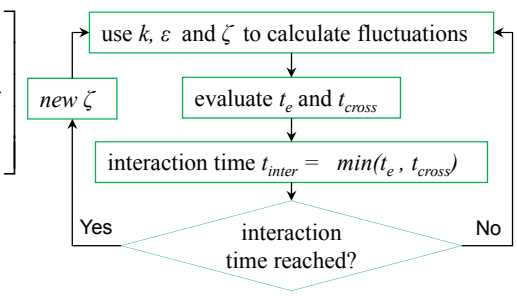




# Simulations and Number of Bubbles Injected

- During the bubble/particle tracking step, 244239 bubbles were injected in each simulation

**Number of Bubbles Tracked**

| Group i | Diameter $d_i$ (mm) | Number $N_i$ |
|---|---|---|
| 1 | 0.025 | 1196 |
| 2 | 0.040 | 1622 |
| 3 | 0.080 | 3589 |
| 4 | 0.100 | 2826 |
| 5 | 0.200 | 8973 |
| 6 | 0.300 | 11521 |
| 7 | 1.000 | 47564 |
| 8 | 2.000 | 80911 |
| 9 | 3.000 | 65022 |
| 10 | 4.000 | 19714 |
| 11 | 5.000 | 1301 |
| | Total | 244239 |

**Casting Conditions**

| Casting Conditions | Value |
|---|---|
| Mold Thickness × Width | 230 × 1300mm |
| Submergence Depth | 160 mm |
| Port Downward Angle | 15 deg. |
| Casting Speed | 1.5 m/min |
| Ar injection | 8.2% vol. |

**List of Simulations**

| | Hook Depth (mm) | $t_{hook}$ (s) | Osc. Frequency (Hz) |
|---|---|---|---|
| A | 0 | - | - |
| B | 3 | 0.25 | 2 |
| C | 6 | 0.25 | 2 |

**Note:**
- **All Simulations are based on the some flow field solution**
- **Case A was old results presented in 2014 CCC annual meeting;**

# Flow field [8]

## (same for all cases in hook study)

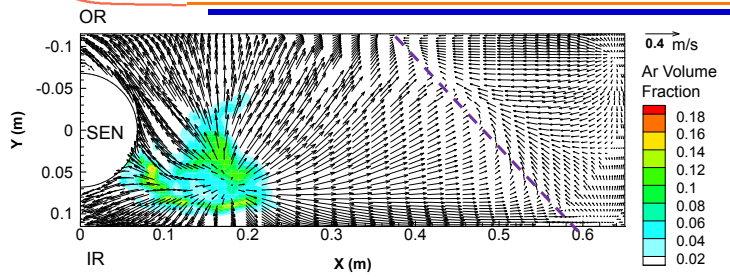


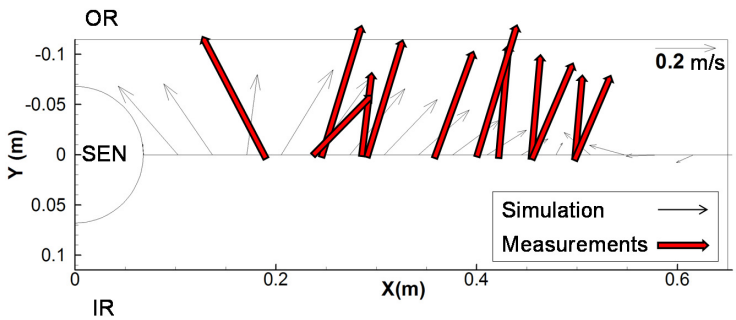


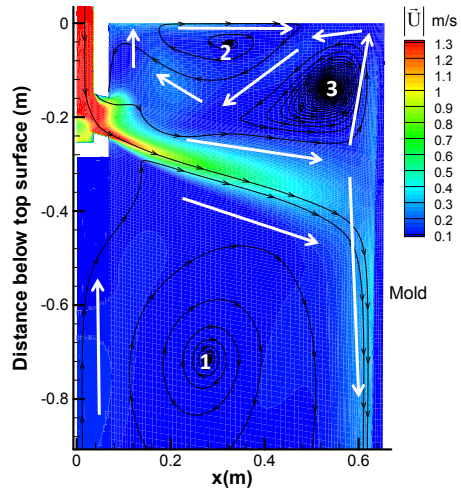


Flow Field[8]

- Predicted cross flow from IR toward OR agrees with the plant measurements
- Cross flow was not observed in the single-phase flow results;
- Plant measurements found even stronger cross flow than predicted;



# WF hook captured bubbles (Hook depth 3mm, Simulation B)

- Reduce hook depth from 6 mm to 3 mm leads to:
  - Less bubbles captured by hook (10~20X less) especially for large bubbles (≥ 1mm);
  - Locations of captured large bubbles are more close to meniscus;
  - On WF, no $d_p$ > 1mm bubbles were capture by hook with 3mm hook depth;

Captured by IR-hook

Captured by OR-hook

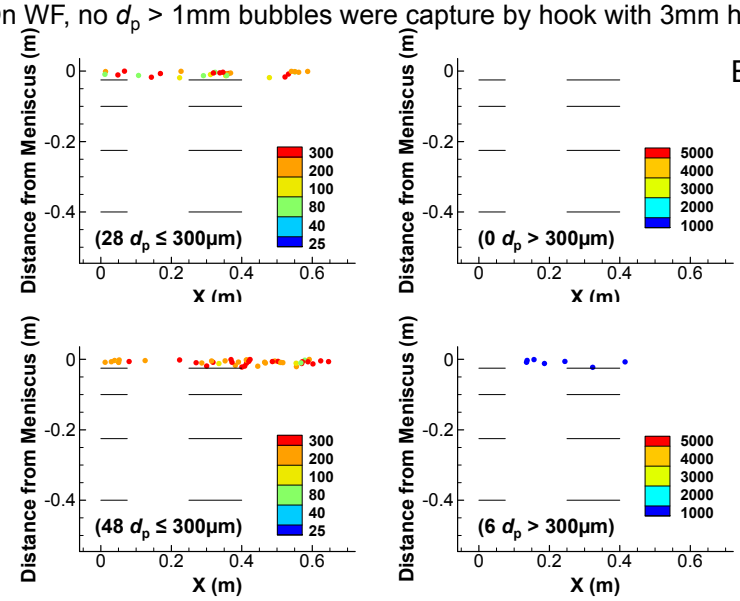


Bubble Diameter (μm)

**Total 28** bubbles capture by IR-hook.

**Total 54** bubbles capture by OR-hook.

# WF hook captured bubbles (Hook depth 6mm, Simulation C)

- Many large bubbles were captured by hook;
- Each "point" representing one captured bubble, but the "point" size is much larger than the real size of the captured bubble, so it looks like the "line" passing through the bubbles, however they may not "visible" to those examined layers because the sliced layer really didn't pass through these tiny bubbles;

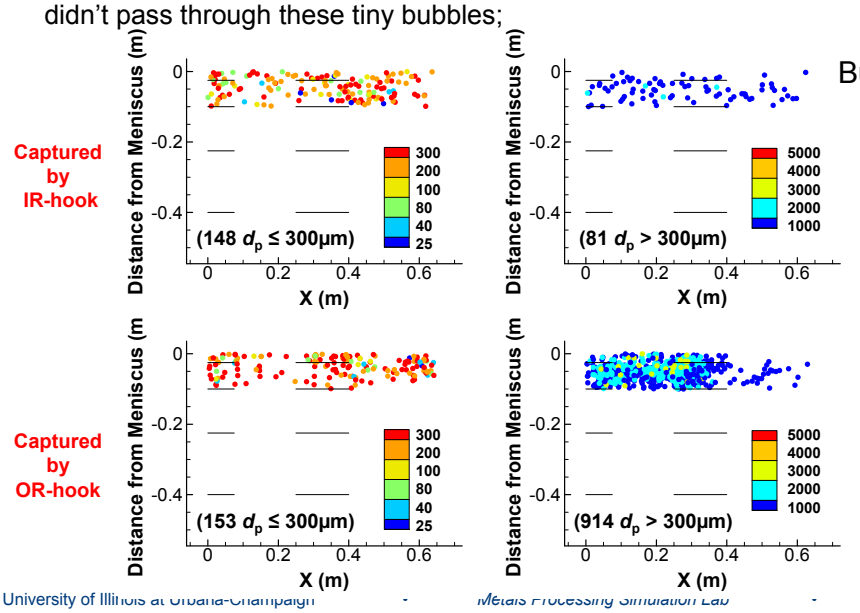


Bubble Diameter (μm)

**Total 229** bubbles capture by IR-hook.

**Total 1067** bubbles capture by OR-hook.



# Captured Small Bubble (d ≤ 0.3mm) on WF/NF and Their Distributions without Hook Capture Mechanism (Simulation A)

- Slide gate open to IR, more capture on IR due to more gas escape from IR side;

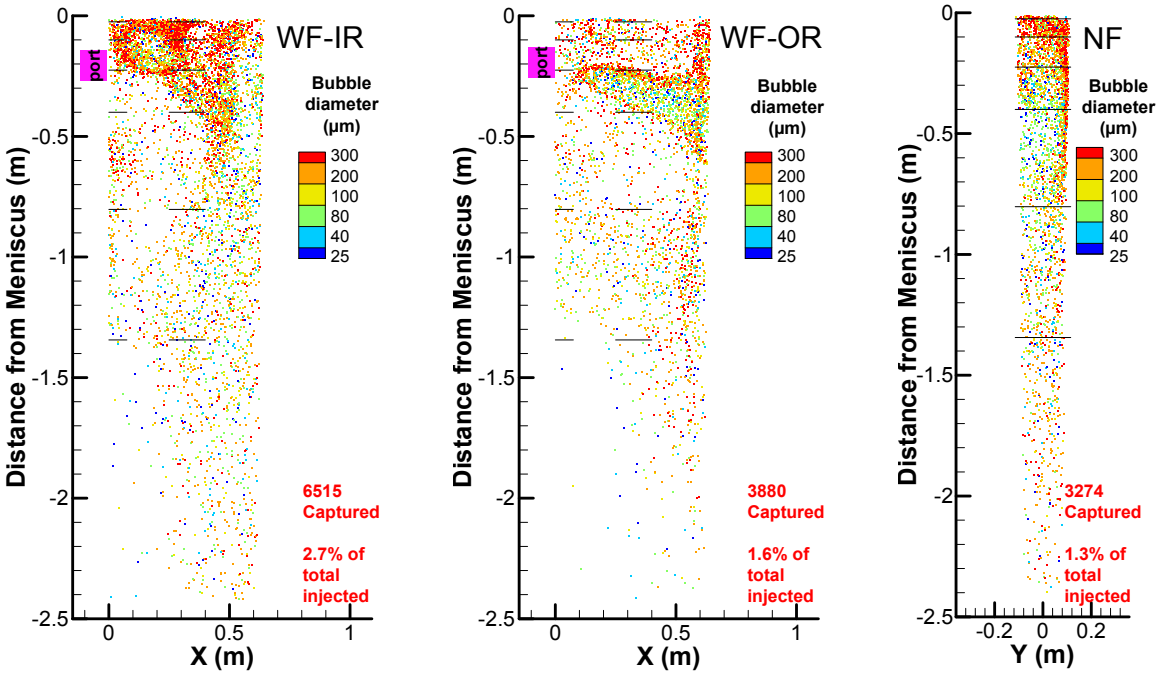

# Capture Small Bubbles (d ≤ 0.3mm) on WF and NF with Hook Depth 3mm Simulation B (Captured by Force Balance and Hook)

- Slide gate open to IR, more capture on IR due to more gas escape from IR side;

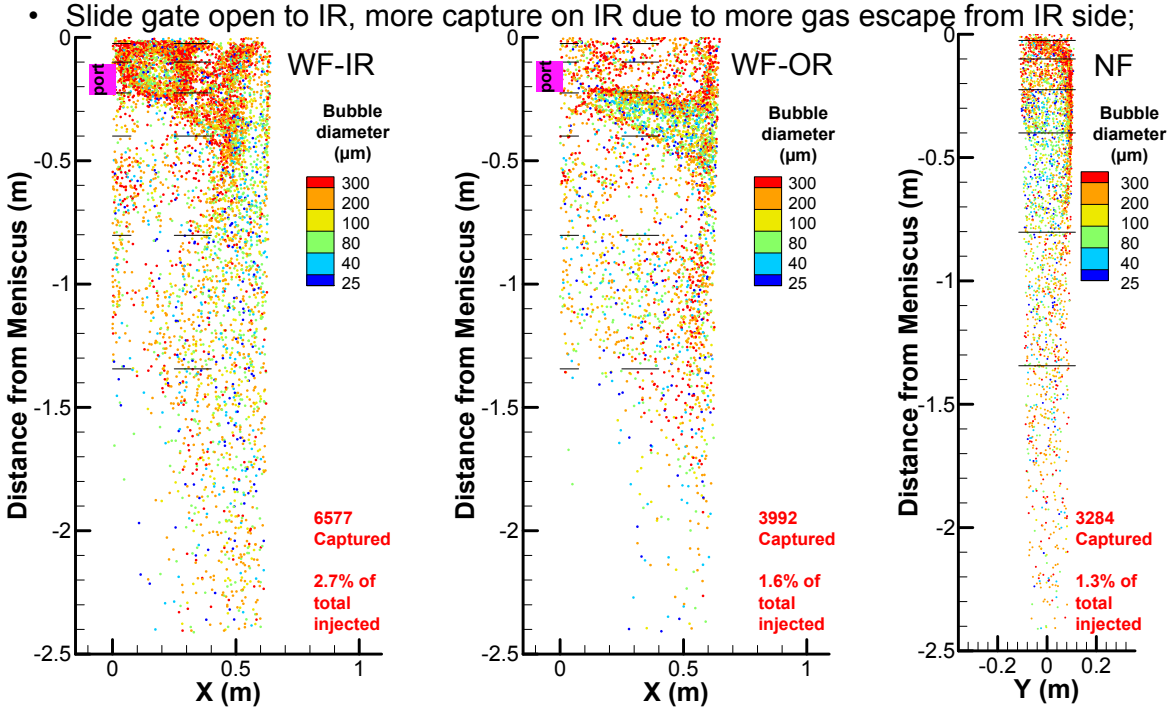




# Capture Small Bubbles (d ≤ 0.3mm) on WF and NF with Hook Depth 6mm Simulation C (Captured by Force Balance and Hook)

- Slide gate open to IR, more capture on IR due to more gas escape from IR side;

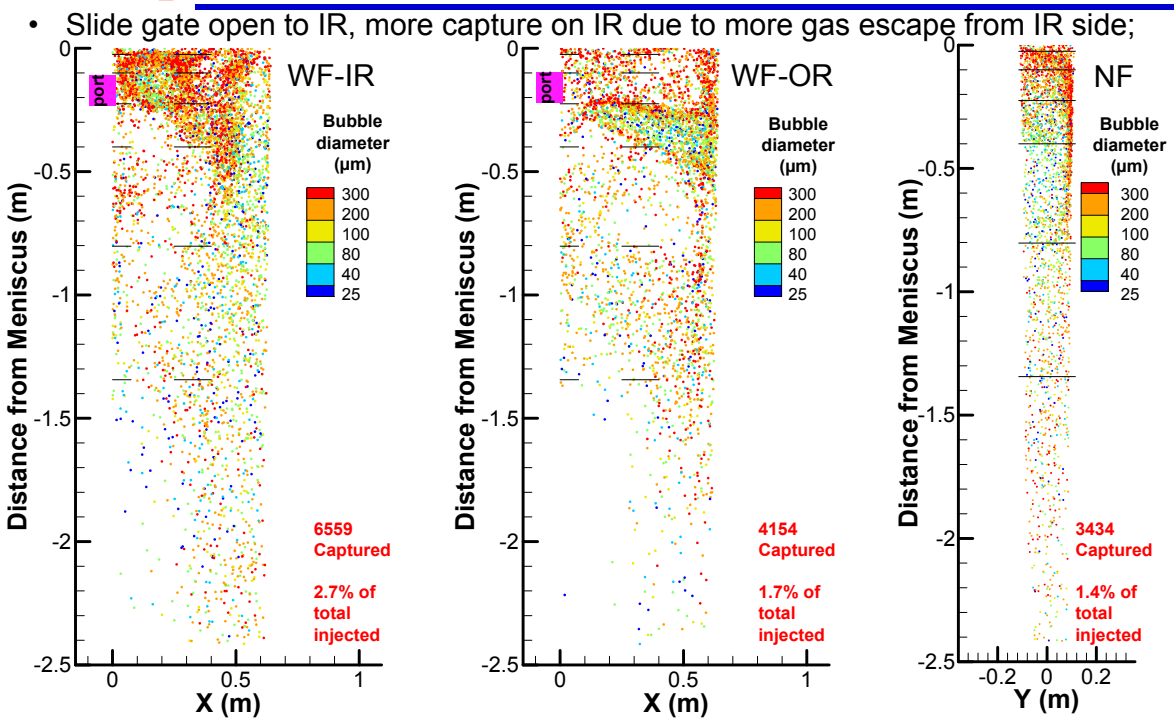

# Effect of Hook Depth on Number of Bubbles Captured (Compare Simulation with Measurements)

Center Region IR

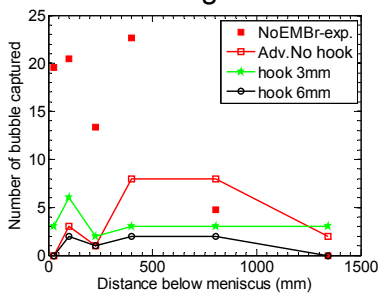


Center Region OR

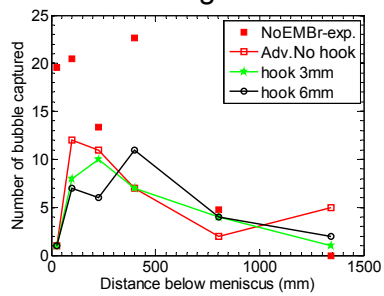


- Number of bubbles captured per sample layer;
- $t_{hook}$ = 0.25s for cases with hook capture mechanism
- Adv. (no hooks) based on average of 10 simulations

Quarter Region IR

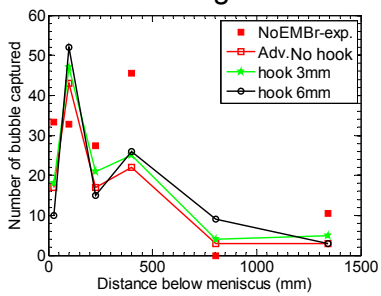


Quarter Region OR

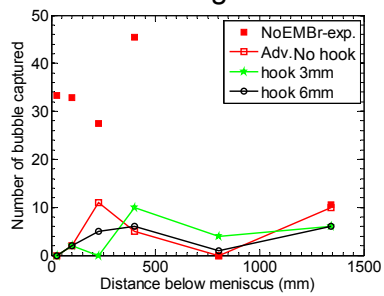


NF

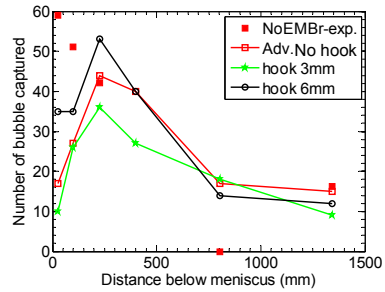




# Effect of Hook Depth on Size of Bubbles Captured (Compare Simulation with Measurements)

Center Region IR

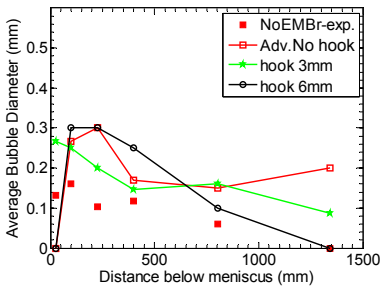


Center Region OR

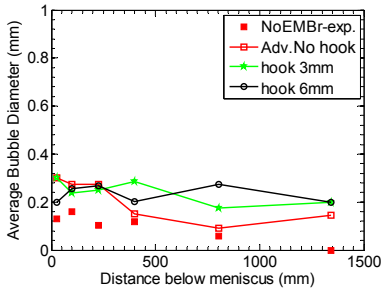


- Size:
  - Average diameter of bubbles captured in each sample layer
- Increasing hook depth: causes larger average diameter in first 2 layers due to more large bubbles captured;

Quarter Region IR

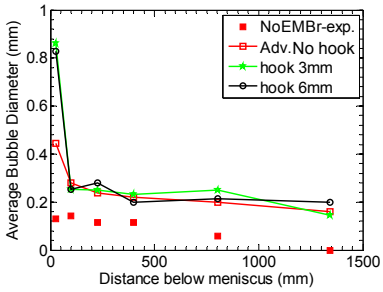


Quarter Region OR

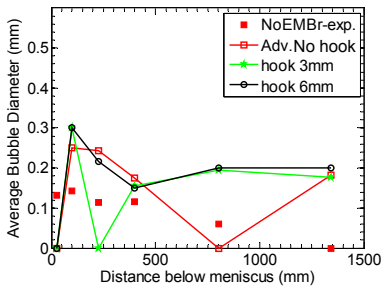


NF

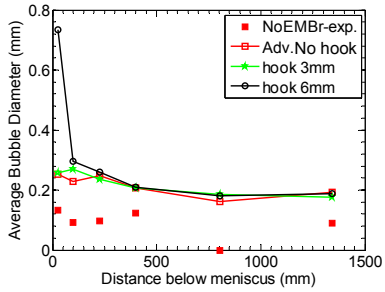

# Effect of Hook Depth on Capture Fraction

| Capture Criteria | Injected all $\Sigma N(d_i)$ | Injected 1mm $N(1\ mm)$ | Captured all $\Sigma n(d_i)$ | Captured 1mm $n(1\ mm)$ | Fraction captured $\varphi(1\ mm)$ | Fraction large $\psi(1\ mm)$ |
|---|---|---|---|---|---|---|
| Simple* No hook[8] | 2,442,390 | 475,640 | 208,944 | 27,799 | 5.84% | **13.3%** |
| Adv. No Hook | 2,442,390 | 475,640 | 137,372 | 432 | 0.09% | **0.3%** |
| Adv. 3mm Hook | 244,239 | 47,564 | 13,939 | 75 | 0.15% | **0.5%** |
| Adv. 6mm Hook | 244,239 | 47,564 | 15,249 | 848 | 1.70% | **5.6%** |
| Experiment | Unknown | Unknown | ~500 | 1 | Unknown | **0.2%** |

*Simple: "touch = capture"

**$\Sigma N(d_i)$:** total number of bubbles injected during the particle tracking step;
**N(1 mm):** number of 1 mm bubbles injected;
**$\Sigma n(d_i)$:** total number of bubbles captured in the entire caster;
**n(1 mm):** number of 1 mm bubbles captured in the entire caster;
**φ(1 mm):** the fraction of 1 mm bubbles that were captured (captured 1mm / injected 1mm);
**ψ(1 mm):** the fraction of captured bubbles that were 1mm diameter (captured 1mm / captured all).

- In all of the measured sample layers, ~500 bubbles were observed; Only one large bubble (1.4 mm diameter) was observed > 0.5 mm. Fraction of captured bubbles with d >1 mm is ψ(1 mm) = 0.2% (1/500).
- Advanced capture criterion prediction of ψ(1 mm) = 0.3% matches plant measurement (0.2%).
- Using 3mm hook depth gives slightly more large bubbles captured;
- Using 6mm hook depth leads to 10X more large bubbles captured near surface;



# Conclusions

- Hook capture mechanism were added into the model and used with advanced capture criterion to predict particle transport and capture
- The model predicted hook captured bubbles were close to meniscus region
- With 3mm hook depth, model predicted 3% more bubbles captured by shell; with 6mm hook, predicted 10% more bubbles captured on WF-OR and NF
- With 6mm hook depth, the model predicted more large bubbles captured by hook which causes larger average bubble diameter
- Effect of hook is not the main reason for predicting less bubbles captured at region close to meniscus

# Future Work

- Hook is not the main reason for predicting less bubbles captured at region close to meniscus, and other effects may need to be investigated (e.g. bubbles/particles reach steel-slag interface may not be removed immediately)

- Use transient LES model and two-way coupled Lagrangian methods to study the transport and capture of particles in the caster under different EMBr conditions.



# Acknowledgments


- Continuous Casting Consortium Members (ABB, AK Steel, ArcelorMittal, Baosteel, JFE Steel Corp., Magnesita Refractories, Nippon Steel and Sumitomo Metal Corp., Nucor Steel, Postech/ Posco, SSAB, ANSYS/ Fluent)
- Xiaoming Ruan and Baosteel at Shanghai, China for plant measurements
- National Science Foundation Grant CMMI-11-30882

# References


[1] Quan Yuan, PhD Thesis, University of Illinois at Urbana-Champaign, 2004.

[2] Sana Mahmood, MS Thesis, University of Illinois at Urbana-Champaign, 2006.

[3] Brian G. Thomas, Quan Yuan, Sana Mahmood, Rui Liu, and Rajneesh Chaudhary, “Transport and Entrapment of Particles in Steel Continuous Casting,” Metall. Mater. Trans. B, 2014, vol. 45, pp. 22–35.

[4] Simon N. Lekakh, Vivek Thapliyal, and Kent Peaslee, in 2013 AISTech Conf. Proc., “Use of an Inverse Algorithm for 2D to 3D Particle Size Conversion and Its Application to Non-Metallic Inclusion Analysis In Steel,” Association for Iron & Steel Technology, Pittsburgh, PA, 2013

[5] Brian Edward Launder and D. B. Spalding, “The Numerical Computation of Turbulent Flows,” Comput. Methods Appl. Mech. Eng., 1974, vol. 3, pp. 269–89.

[6] Saj Morsi and A. J. Alexander, “An Investigation of Particle Trajectories in Two-Phase Flow Systems,” J. Fluid Mech., 1972, vol. 55, pp. 193–208.

[7] A. D. Gosman and E. Loannides, “Aspects of Computer Simulation of Liquid-Fueled Combustors,” J. Energy, 1983, vol. 7, pp. 482–90.

[8] K. Jin, B. G. Thomas, R. Liu, S. P. Vanka, and X. M. Ruan, “Simulation and Validation of Two-Phase Turbulent Flow and Particle Transport in Continuous Casting of Steel Slabs,” IOP Conf. Ser. Mater. Sci. Eng., 2015, vol. 84, p. 012095.